NJC

Accepted Manuscript

This is an *Accepted Manuscript*, which has been through the Royal Society of Chemistry peer review process and has been accepted for publication.

Accepted Manuscripts are published online shortly after acceptance, before technical editing, formatting and proof reading. Using this free service, authors can make their results available to the community, in citable form, before we publish the edited article. We will replace this *Accepted Manuscript* with the edited and formatted *Advance Article* as soon as it is available.

You can find more information about *Accepted Manuscripts* in the Information for Authors.

Please note that technical editing may introduce minor changes to the text and/or graphics, which may alter content. The journal's standard Terms & Conditions and the Ethical guidelines still apply. In no event shall the Royal Society of Chemistry be held responsible for any errors or omissions in this *Accepted Manuscript* or any consequences arising from the use of any information it contains.

ROYAL SOCIETY OF CHEMISTRY

www.rsc.org/njc

Development of halogen free flame retardant phosphazene and rice husk ash incorporated benzoxazine blended epoxy composites for microelectronic applications

Krishnamoorthy Krishnadevi and Vaithilingam Selvaraj *

Nanotech research lab, Department of Chemistry, University College of Engineering-Villupuram (A Constituent College of Anna University, Chennai), Kakuppam, Villupuram-605 103, Tamil Nadu, India.

Abstract

The present work is focused on the synthesis and characterization of flame retardant amine terminated cyclophosphazene and silane functionalized rice husk ash reinforced benzoxazine blend epoxy composites as a halogen free flame retardant material (ATCP/FRHA/Bz-Ep). FT-IR spectroscopy, scanning electron microscope (SEM), X-ray diffraction analysis, contact angle measurements, dielectric constant, DSC, TGA, UL-94, LOI and cone calorimeter were used to characterize the structural, surface morphology, electrical, thermal and flame retardant properties of resultant ATCP/FRHA/Bz-Ep composite material. The experimental results suggested that ATCP/FRHA/Bz-Ep composites exhibit better flame retardant and dielectric performance compared to that of neat Bz-Ep material. A plausible mechanism of fire retardant ATCP/FRHA/Bz-Ep composite material is hypothesized based on the results of cone calorimetric, thermal and electrical analysis. From the above results, it was concluded that the ATCP/FRHA/Bz-Ep composite can be used as electrical resistant material for electronic and microelectronic applications.

Key words: Benzoxazine, epoxy, cyclophosphazene, flame retardant, rice husk ash, dielectric constant

***Corresponding Author**: V. Selvaraj, rajselva_77@yahoo.co.in, vselva@aucev.edu.in (V. Selvaraj) Fax: 04146-224500

Introduction

Polymer composites are light weight materials that can be used various high performance application, which are required as an essential and desirable properties for sustainable flame retardant polymers. Flame retardants are one of the most important additives for combustible polymers to improve their fire resistance properties [1-3]. So, the flame retardant materials are used to reduce combustibility of the polymers and toxic fume production, which are pivotal part of the development and applications of new materials.

Epoxy resins are high performance thermosetting resins possessing many attractive properties such as high mechanical, good adhesion [4], good electrical insulation properties [5], low cost and ease of forming etc. [6]. However epoxy resins are easily flammable and they are unable to satisfy for some high performance flame retardant applications. Generally, the flame retardant property of epoxy resins can be improved by adding flame retardant additives or by incorporating reactive flame retardants.

The most effective flame retardants are the halogen containing chemicals, but they are usually releasing harmfully toxic gases as well as heavy smoke during combustion process. Though the halogen containing flame retardants attract great attention, but still it requires significant challenge in both academic and industrial applications. However, especially brominated flame retardants are restricted in many countries due to the migration of toxic by-products such us hydrogen halides and dioxins [7] to the environment during combustion process.

The above draw backs are tempting the researchers to develop innovative and eco friendly halogen free polymeric materials for electronic, electrical, aerospace and transportation applications. Among all halogen free flame retardants, scientists are introducing nitrogen, phosphorous and silica based intumescent flame retardants as additives for achieving flame retardant performance.

Due to prominent processability, excellent thermal and mechanical properties of epoxy modified benzoxazine blended systems have been attracted more and more attention in wide range of application including adhesives; filler reinforced composite materials, and coatings for electronic circuits [8-11]. However, the absences of inorganic materials in the benzoxazine blended epoxy systems have low flame retardant capacities that are unsatisfying the fire resistance properties of the materials. So, the effective and eco-friendly inorganic flame retardant materials should be incorporated in the Bz-Ep composites in order to enhance the flame resistance properties. Rice husk ash is a biomass waste material, and it contains a rich source of silica. In general, utilization of biomass rice husk ash in the composites have attributed to several advantages such as low density, greater deformability, less abrasiveness to equipment, biodegradability and low cost. Hence, the present work attempted to get low k values, high performance flame retardant, improved thermal and flame retardant properties, improved hydrophobic etc., by using eco friendly bio waste materials like rice husk ash.

Phosphazenes are well known class of versatile functional materials having an inorganic backbone structure. When the phosphazenes are appropriately substituted, the resultant materials can be employed as flame resistant materials, elastomers, memberanes, solid ionic conductors and inert biomaterials [12]. Such compounds containing both phosphorous and nitrogen can display enhanced flame retardancy when compared to similar compounds containing phosphorous alone. In addition, these materials yield relatively minor amounts of toxic combustion products in fire situations. So, the properties of organic polymers can be modified to improve significantly their fire resistance, ionic conductivity and biological compatibility by the incorporation of small amount of specially modified eco-friendly phosphazene [13-15]. Hence, this makes phosphazene particularly good candidates for the development of fire resistance eco-friendly materials in electrical and electronic applications.

With these view in mind, the present work is focused on the synthesis and characterization of ATCP/FRHA/Bz-Ep composites for flame retardant applications. The improved thermal properties of ATCP/FRHA/Bz-Ep composites were confirmed by TGA and DSC techniques. The flame retardant properties of synthesized composites were studied by UL-94 test, LOI and cone calorimeter measurements. Further, the dielectric and hydrophobic nature of the composites are determined by BDS and contact angle measurements, respectively. From the result, it was concluded that the presence of N, P and silica (three in one) material can promote thermal, flame retardant, dielectric (low k) and hydrophobic properties,

METHODS AND MATERIALS

Hexachlorocyclotriphosphazene (CP) and 3-aminopropyltrimethoxysilane (3-APTMS) (99%) were purchased from Sigma Aldrich, India. Diglycidyl ether of bisphenol-A epoxy resin (LY556) (DGEBA) was purchased from Ciba-Geigy Ltd., India. 4-acetamido phenol, bisphenol-A, triethyl amine, potassium carbonate, aniline, sodium hydroxide, paraformaldehyde and other solvents (AR grade) were purchased from SRL Chemicals, India.

Synthesis of hexa(acetamidophenyl)cyclotriphosphazene (CPAC)

A mixture of 4-acetamido phenol (15.65 g, 0.1035 mol) and K_2CO_3 (21.09 g, 0.15824 mol) in dry acetone (200 ml) were effectively agitated at room temperature for 30 minutes. To this mixture, hexachlorocyclotriphosphazene (CP) (5g, 0.0143 mol) was added and refluxed at 60°C for 4 days. Then, the resulted product was cooled to room temperature and filtered. The crude product (CPAC) was further purified by using hexane and dried in a vacuum oven at 50 °C for 2 h. The yield of the product and melting point were found to be 62.95% and 252-255 °C, respectively.

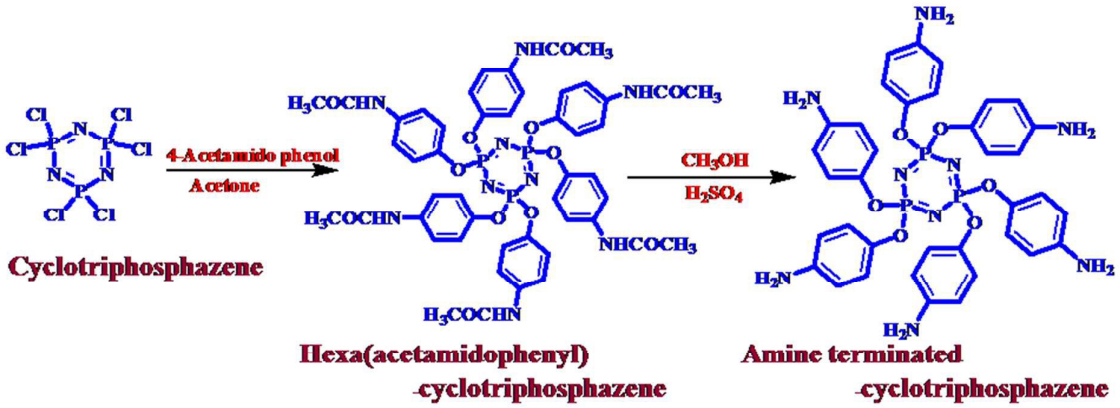

Figure 1. Synthesis of amine terminated cyclotriphosphazene.

Synthesis of amine terminated cyclophosphazene (ATCP)

A mixture of hexa(acetamidophenyl)cyclotriphosphazene (CPAC) (9 g), methanol (180 ml) and sulfuric acid (108 ml) are refluxed for 4 h at 80 °C and then cooled to room temperature followed by the addition of ammonia in drop by drop under ice bath until the P^H reaches to 8. The resultant grey color solid product (Figure 1) is filtered, washed with excess of water and dried in vacuum at 50 °C for 48 h. The yield of the product and melting point were found to be 90% and 172–174 °C, respectively.

Preparation of rice husk ash

Rice husk was collected from a local rice mill in Tamilnadu, India and washed several times with de-ionized water. It was dried in sun light for 7 days. The dried rice husk was burned in an open air. After burning, the residue was crushed to obtain rice husk ash (RHA). The crushed rice husk ash (40 g) was immersed in 1M HCl (1 liter) solutions for 4 h. The rice husk ash was washed repeatedly with deionized water and then dried in an oven at 110°C for 2 days. Rice husk ash was calcinated (in a ceramic crucible) at 350°C for 3 h and 600°C for 4 h in a muffle furnace. The resultant rice husk ash is white in color and stored for further use.

Functionalization of RHA

RHA silica is functionalized with 3-aminopropyltrimethoxysilane (3-APTMS) according to the reported method [16]. 50 g of rice husk ash was mixed with 400 ml of dried toluene. The mixture was refluxed under nitrogen atmosphere for 2 h and then 20 ml of 3-aminopropyltrimethoxysilane (3-APTMS) was slowly added. Finally the resultant product was filtered, washed with ethanol and dichloromethane for several times and then dried at 25°C for 24 h. The resultant functionalized rice husk ash (FRHA) was stored for further use (Figure 2).

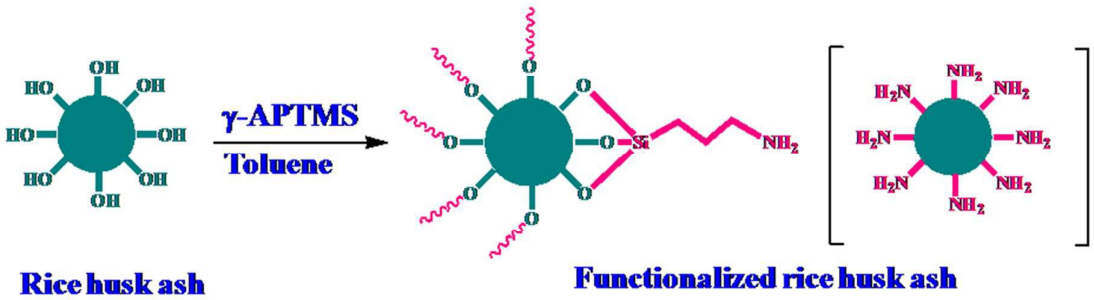

Figure 2. Synthesis of functionalized rice husk ash.

Synthesis of flame retardant composites

According to our previous report, 15 wt.% of CPA (hexa(aminophenyl) cyclotriphosphazene) is more effective than the other weight percentage ratios [17, 18]. Hence, DGEBA epoxy resin and benzoxazine (Bz) [19] were mixed with 15 wt.% of amine terminated cyclotriphosphazene and various weight percentage (1,3 and 5%) of functionalized rice husk ash (**Table 1**). The resultant reaction mixture was agitated for 5 h using mechanical stirrer. The amine terminated cyclophosphazene, silane functionalized rice husk ash, benzoxazine and epoxy material (ATCP/FRHA/Bz-Ep) composites (**Figure 3)** were thoroughly mixed and then cured using preheated mould at 120°C for 1 h, 180°C for 1 h and 250°C for 2 h in order to get ATCP/FRHA/Bz-Ep composites**.**

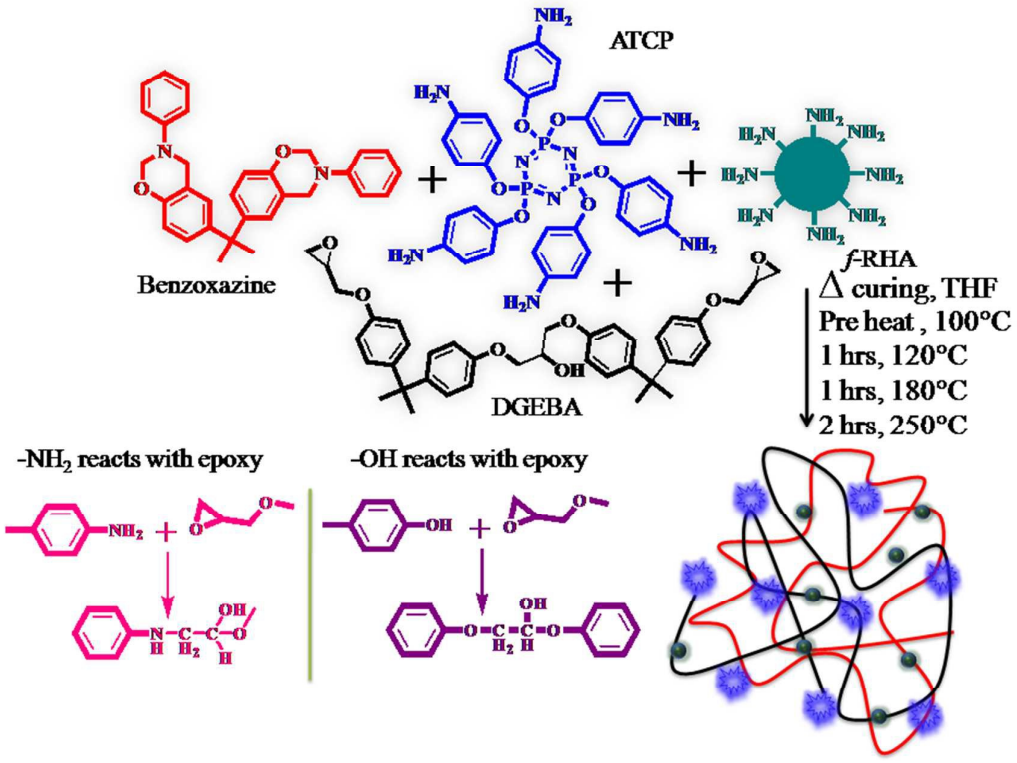

Figure 3. Proposed schematic representation of amine terminated cyclophosphazene and functionalized rice husk ash reinforced benzoxazine blend epoxy composites.

Table 1

Preparation of amine terminated cyclophosphazene and functionalized rice husk ash based flame retardant (ATCP/FRHA/Ep-Bz) composites.

Sample code	ATCP (g)	FRHA (g)	Bz (g)	Ep (g)	THF (ml)
Bz-Ep		-	50	50	20
ATCP/Bz-Ep	15	-	42.5	42.5	20
ATCP/FRHA(1%)/Bz-Ep	15	1	42	42	20
ATCP/FRHA(3%)/Bz-Ep	15	3	41	41	20
ATCP/FRHA(5%)/Bz-Ep	15	5	40	40	20

Characterization

FT-IR spectra were recorded on Perkin Elmer 6X spectrometer. The surface morphologies of the samples were examined using scanning electron microscope (SEM;

JEOL JSM Model 6360). X-ray diffraction patterns were recorded at 25°C by using Rich Seifert, Model-3000 X-ray powder diffractometer (monitoring the diffraction angle at 2θ from 10° to 70°). Thermogravimetric analysis (TGA) is performed on Netzsch STA 409 thermogravimetric analyzer under a continuous flow of nitrogen (20 mL/min) at a heating rate of 10 °C/min. Differential scanning calorimetric analysis (DSC) was performed on a Netzsch DSC-200. The samples (about 10 mg in weight) were heated from 25°C to 500 °C and the thermograms were recorded at a heating rate of 10 °C/min. The dielectric constant and dielectric loss of the samples were measured using a Broad band dielectric spectrometer (BDS- NOVOCONTROL Technologies, Germany) at 35°C in the frequency range from 1Hz to 2 MHz. Contact angle measurements were carried out by goniometer using sessile drop method. Before measuring the contact angle, the samples should be dried at 60°C in a vacuum oven for 24 h. The vertical burning tests were carried out using a UL-94 vertical flame chamber instrument with sample dimension of 130 × 13 × 3 mm according to the ASTM D3801. The limiting oxygen index (LOI) was analyzed with sample dimension 150 × 37.5 × 12 mm using Atlas HVUL2 according to ASTM D2863. The cone calorimeter tests were conducted following the ISO 5660 procedures on a cone calorimeter (Fire Testing Technology Ltd.). Specimens [dimension: 100 × 100 × 2.9 (± 0.1) mm^3] were irradiated with a heat flow of 50 kW/m^2. From this analysis, the time to ignition (TTI), heat release rate (HRR), total heat release (THR), total smoke production (TSP), char residues, and CO/CO_2 emission rate ratio can be acquired.

Results and discussions

Structural characterization

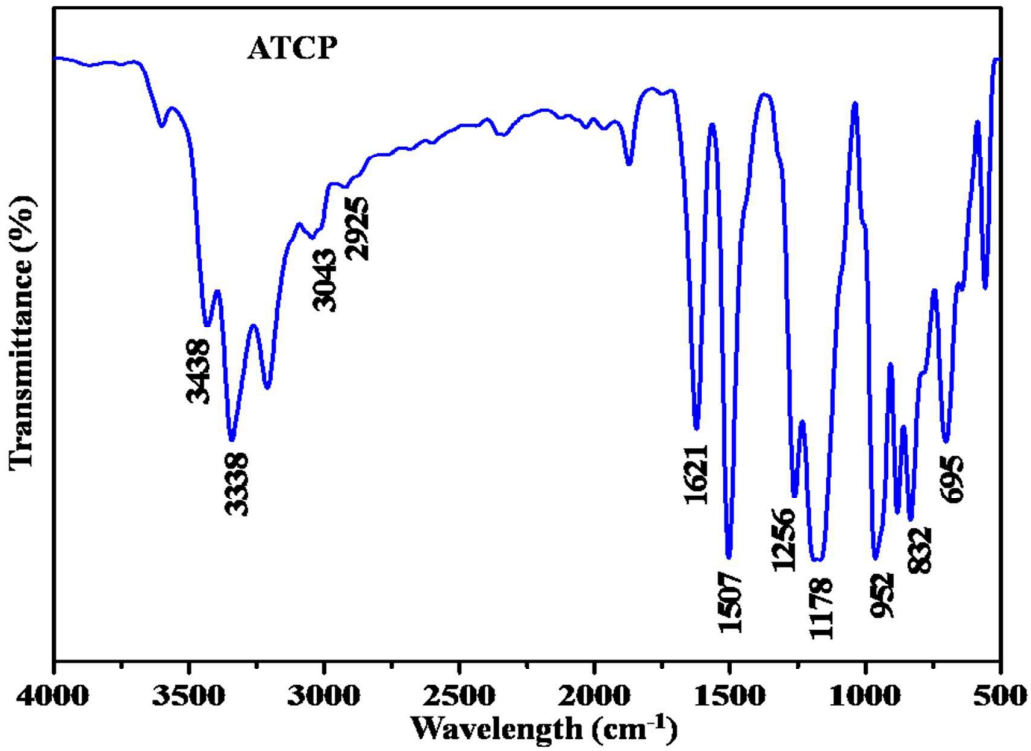

Figure 4. FT-IR spectrum of amine terminated cyclophosphazene (ATCP).

The two broad band's observed at 3438 and 3338 cm^{-1} were corresponding to -NH_2 stretching vibrations, in fact they are also ascertain the presence of amine group in ATCP material (**Figure 4**). The peaks observed at 3043 and 2925 cm^{-1} were corresponding to ring C-H stretching vibrations. The aromatic C-C stretching vibrations were noticed at 1507 and 1621 cm^{-1}. The characteristic stretching vibrations of P-O-Ph, P-N-P and P-O-C were visualized at 1256, 1178 and 952 cm^{-1} respectively. The aromatic C-H bending vibrations were appeared at 832 and 695 cm^{-1}.

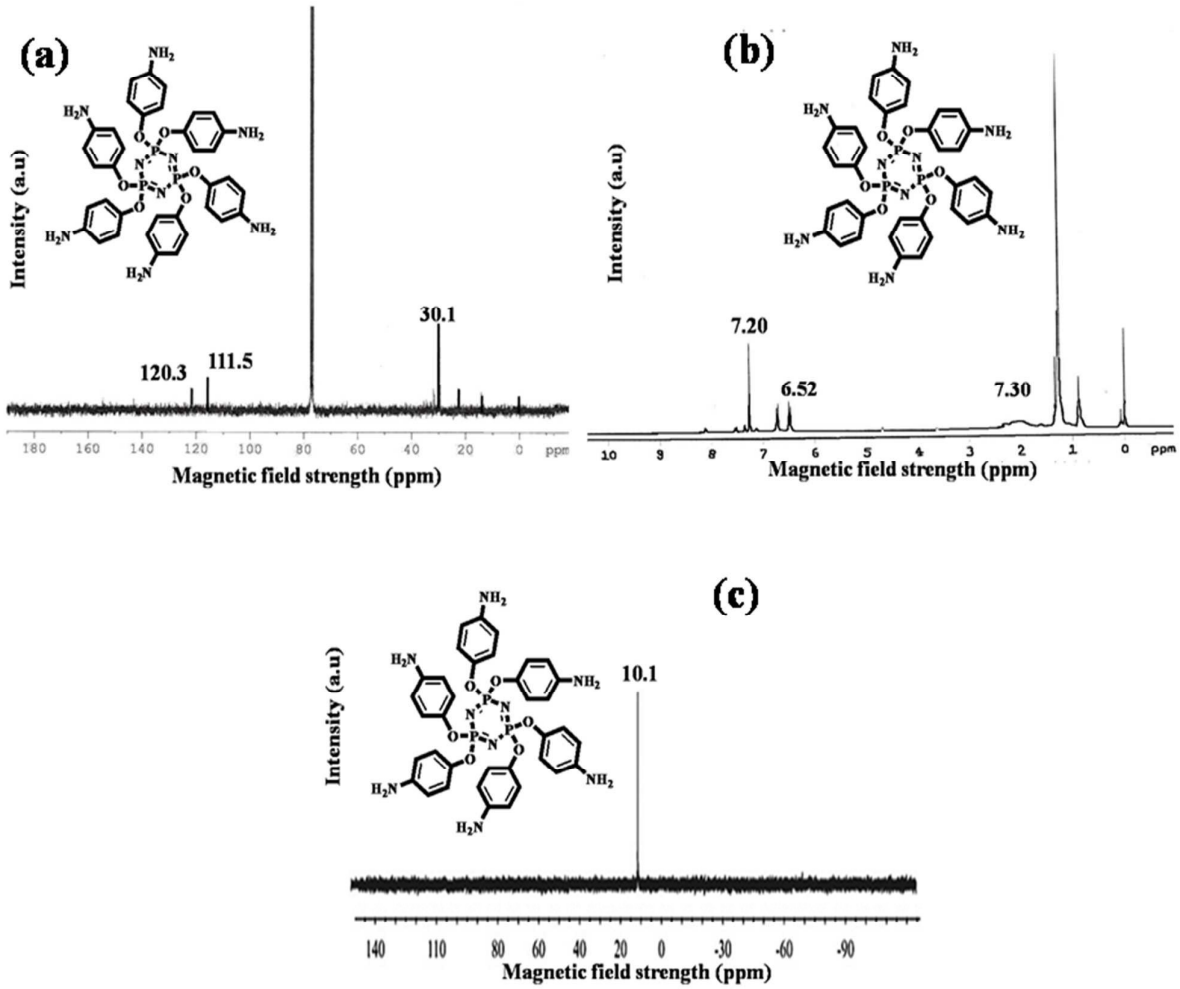

Figure 5. ^{13}C NMR (a), ^{1}H NMR (b) and ^{31}P NMR (c) spectra of synthesized ATCP.

In the ^{13}C NMR spectrum (**Figure 5(a)**, the presence of aromatic carbon was confirmed by the peaks observed at 111.5 and 120.3 ppm. From ^{1}H NMR spectrum (**Figure 5-b**), the presence of aromatic protons in ATCP was confirmed by the appearance of the peaks at 6.52 and 7.2 ppm. The presence of NH_2 protons was confirmed by the peak obtained at 2.3 ppm. The appearance of peak at 30.1 confirms the presence of carbon that was attached to NH_2 group in ATCP material. Single peak appeared at 10.1 ppm in ^{31}P NMR spectrum (**Figure 5(c)** confirms the presence of phosphorous in ATCP material.

Figure 6 shows the FT-IR spectra of rice husk ash and functionalized rice husk ash. The peak observed at 3473 cm^{-1} indicates the presence of both hydrogen bonded -OH group

and Si-OH group. The Si-OH stretching vibration was appeared due to both the silanol group and adsorbed water on the surface [20]. Similarly, the peak observed at 2937 cm^{-1} indicates the presence of -CH_2 stretching vibration. The peaks appeared at 1095 and 800-798 cm^{-1} confirm the presence of Si-O-Si bond. Thus, these results evidence that the aminopropyl groups have become an integral point of RHA and it was covalently bonded with RHA material.

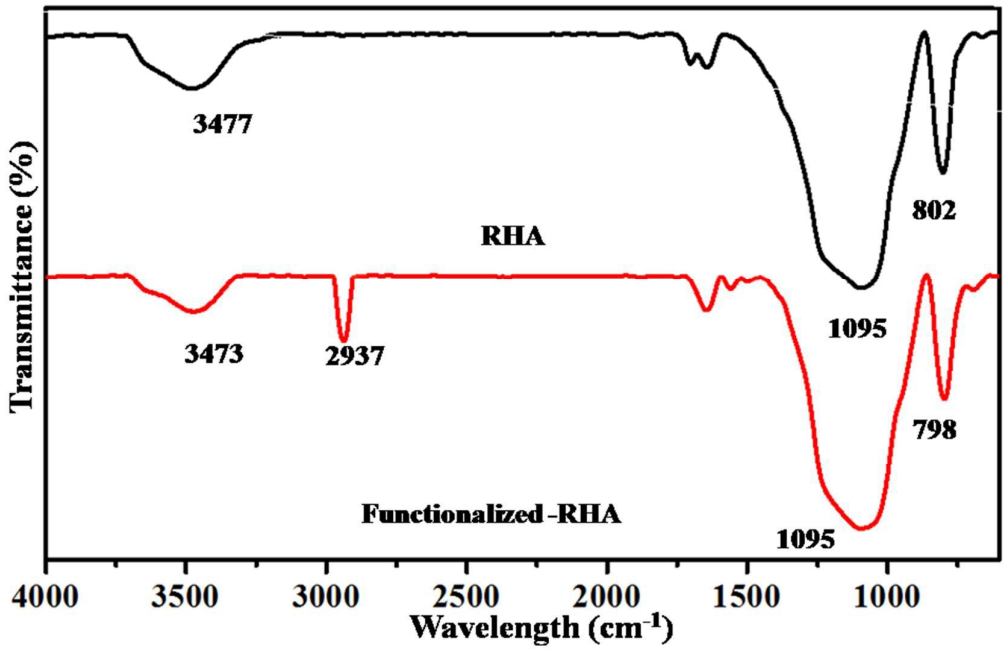

Figure 6. FT-IR spectra of rice husk ash and functionalized rice husk ash materials.

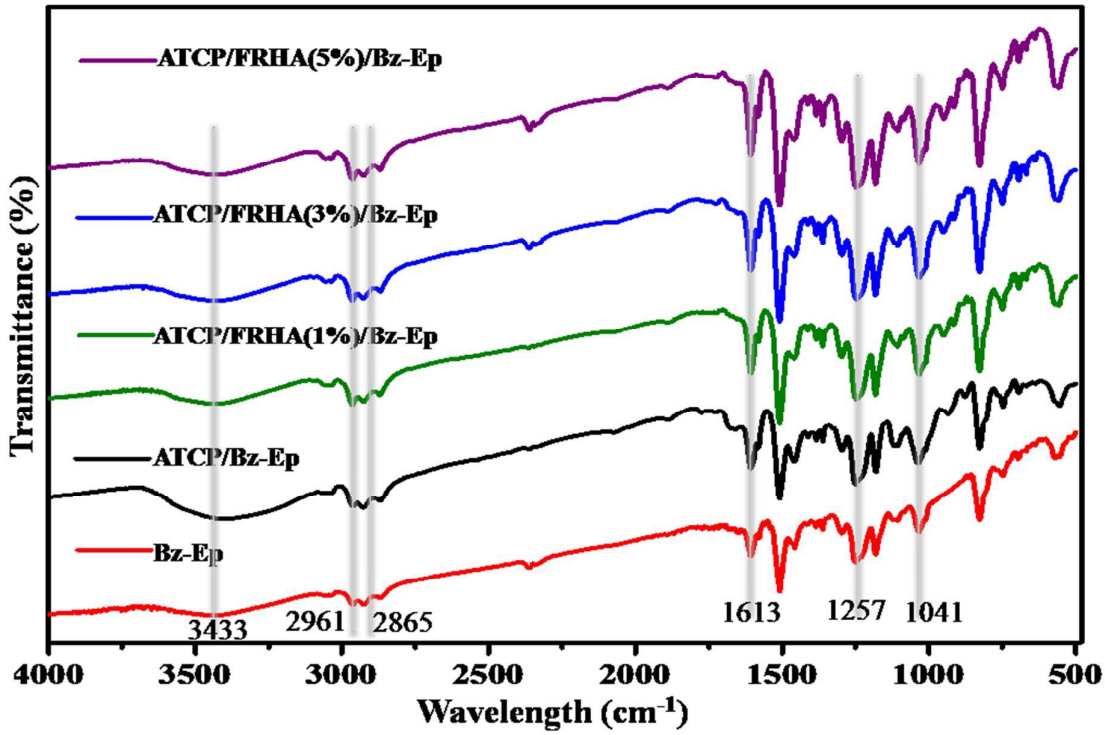

Figure 7. FT-IR spectra of Bz-Ep, ATCP/Bz-Ep, ATCP/FRHA(1%)/Ep-Bz, ATCP/FRHA(3%)/Bz-Ep and ATCP/FRHA(5%)/Bz-Ep flame retardant composites.

The FT-IR spectra of Bz-Ep, ATCP/Bz-Ep, ATCP/FRHA(1%)/Bz-Ep, ATCP/FRHA(3%)/Bz-Ep and ATCP/FRHA(5%)/Bz-Ep composites were shown in **Figure 7**. The peaks observed at 3433 cm-1 were corresponding to OH stretching vibrations. The stretching band observed at 2961 and 2865 cm^{-1} were corresponding to C-H stretching vibrations. The peak observes at 1041 cm^{-1}confirms the presence of C-O stretching vibrations. The aromatic C-C stretching vibrations were observed at 1514 and 1613 cm^{-1}. The characteristic stretching vibrations of P-O-Ph, P-N-P and P-O-C were observed at 1257 cm^{-1}, 1186 cm^{-1} and 946 cm^{-1}, respectively. The peak at 827 cm^{-1} confirms the presence of aromatic C-H bending vibrations. The Si-O-Si peak was observed at 1000 - 1130 cm^{-1}. The above results confirm the complete curing of ATCP/FRHA/Bz-Ep composites.

Surface morphology

From the SEM image of Bz-Ep composite [**Figure 8(a)],** it was noticed that the synthesized composite material have homogeneous glassy microstructure

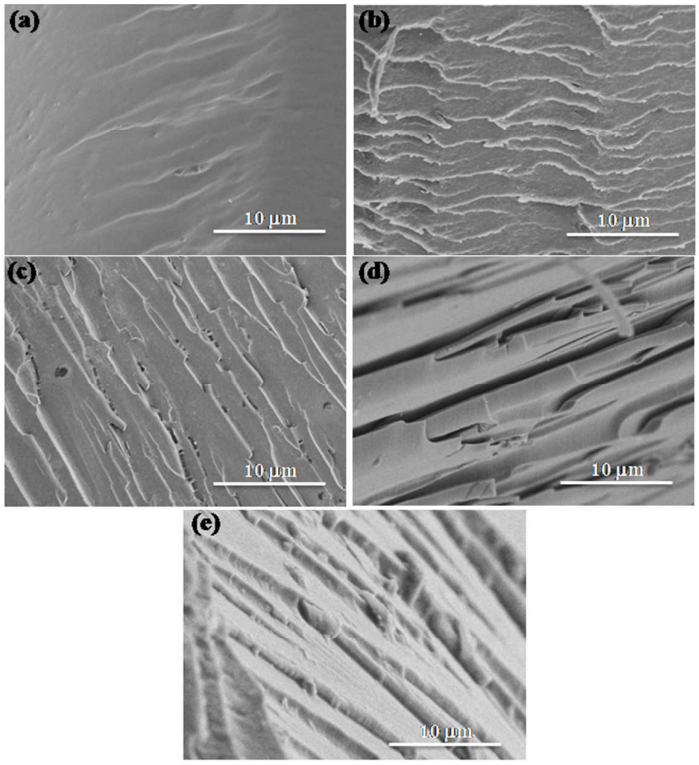

Figure 8. Fracture morphology of Bz-Ep (a), ATCP/Bz-Ep (b), ATCP/FRHA(1%)/Bz-Ep (c), ATCP/FRHA(3%)/Bz-Ep (d) and ATCP/FRHA(5%)/Bz-Ep (e) composites.

Further, the ATCP/Bz-Ep/FRHA composite **[Figure 8(b-e)]** shows a platelet-like surface morphology and exhibited the nonphase separated homogeneous morphology owing to crosslink among benzoxazine based epoxy resin with amine terminated cyclophosphazene and functionalized rice husk ash materials.

X-ray diffraction analysis

The X-ray diffraction studies were used to ascertain the structural modification of Bz-Ep, ATCP/Bz-Ep, ATCP/FRHA(1%)/Bz-Ep, ATCP/FRHA(3%)/Bz-Ep and ATCP/FRHA (5%)/Bz-Ep composites. The resultant XRD patterns of synthesized composites were shown in **Figure 9**. The cured composites almost have the similar prominent peaks at an angle of

about 17.95°, which is characteristics of amorphous [21, 22] composites corresponding to the interaction of d spacing at 4.9 Å calculated from the Bragg's equation ($\lambda = 2\ d \sin\theta$). Hence, the XRD studies confirm the complete incorporation of flame retardant additive like ATCP and FRHA material in the Bz-Ep blends.

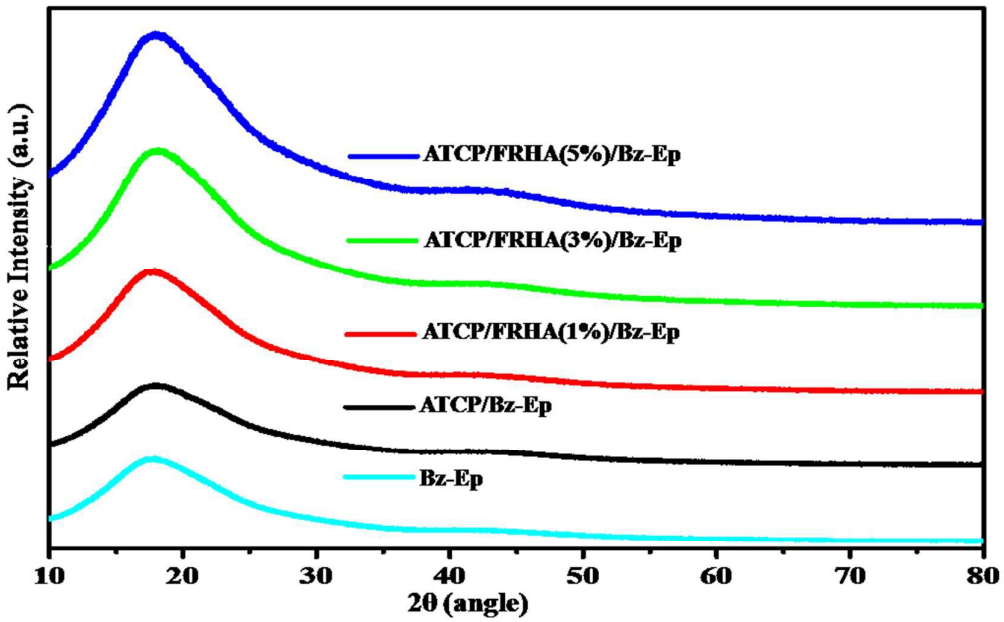

Figure 9. XRD analysis of Bz-Ep, ATCP/Bz-Ep, ATCP/FRHA(1%)/Bz-Ep, ATCP/FRHA(3%)/Bz-Ep and ATCP/FRHA(5%)/Bz-Ep flame retardant composites.

Contact angle measurements

The wettability of Bz-Ep, ATCP/Bz-Ep, ATCP/FRHA(1%)/Bz-Ep, ATCP/FRHA (3%)/Bz-Ep and ATCP/FRHA(5%)/Bz-Ep composites were determined through the contact angle measurements by using goniometer. The surface contact angles were measured with 5 µl of water as the probe liquid and the results were presented in **figure 10**. The values of contact angle of Bz-Ep, ATCP/Ep-Ep, ATCP/FRHA(1%)/Bz-Ep, ATCP/FRHA(3%)/Bz-Ep and ATCP/FRHA(5%)/Bz-Ep composites are 68°, 82°, 86°, 98° and 106°, respectively. From the results, it was noticed that the hydrophobic nature can be increased with the addition of phosphazene and various percentage of functionalized rice husk ash in the Bz-Ep composite.

This is due to less polar nature of Si-O-Si linkages in the network system, which increases the hydrophobic nature of the resulting hybrid systems.

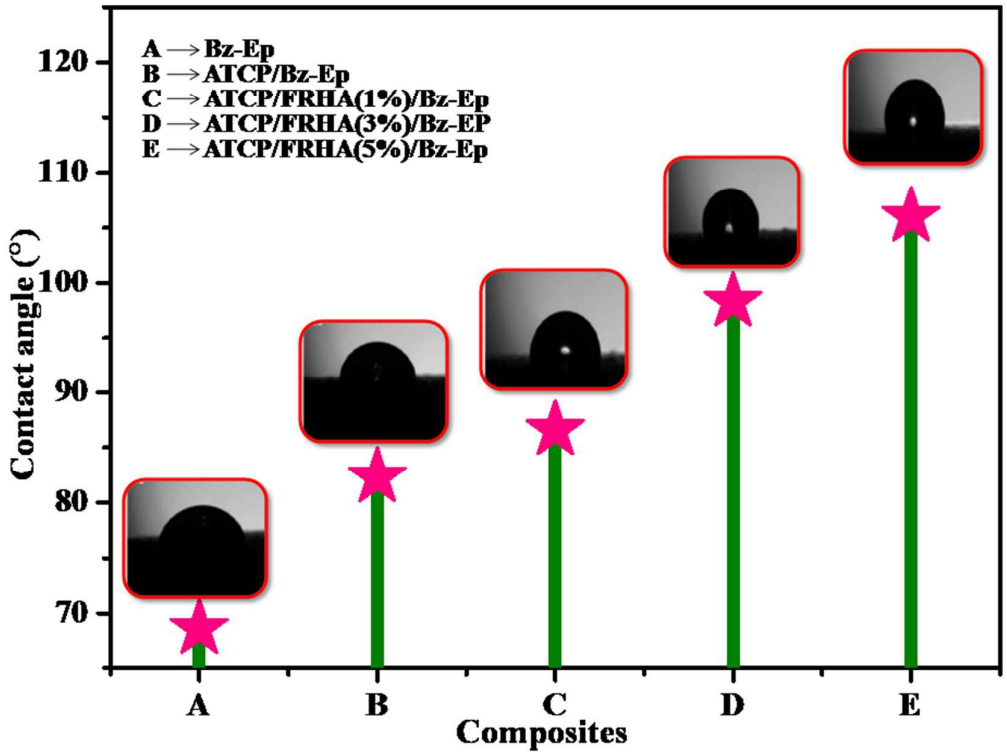

Figure 10. Contact angle measurements of Bz-Ep, ATCP/Bz-Ep, ATCP/FRHA(1%)/Bz-Ep, ATCP/FRHA(3%)/Bz-Ep and ATCP/FRHA(5%)/Bz-Ep flame retardant composites.

Dielectric properties

The dielectric constants with respect to the applied AC frequencies ranging from 1 MHz to 20 MHz were presented in **Figure 11**. The obtained dielectric constant and dielectric loss values were given in **Table 2**. From **Figure 11,** it was noticed that the ATCP/FRHA(5%)/Bz-Ep hybrid has lower value of dielectric constant ~1.62 than that of Bz-Ep (~4.63) composite.

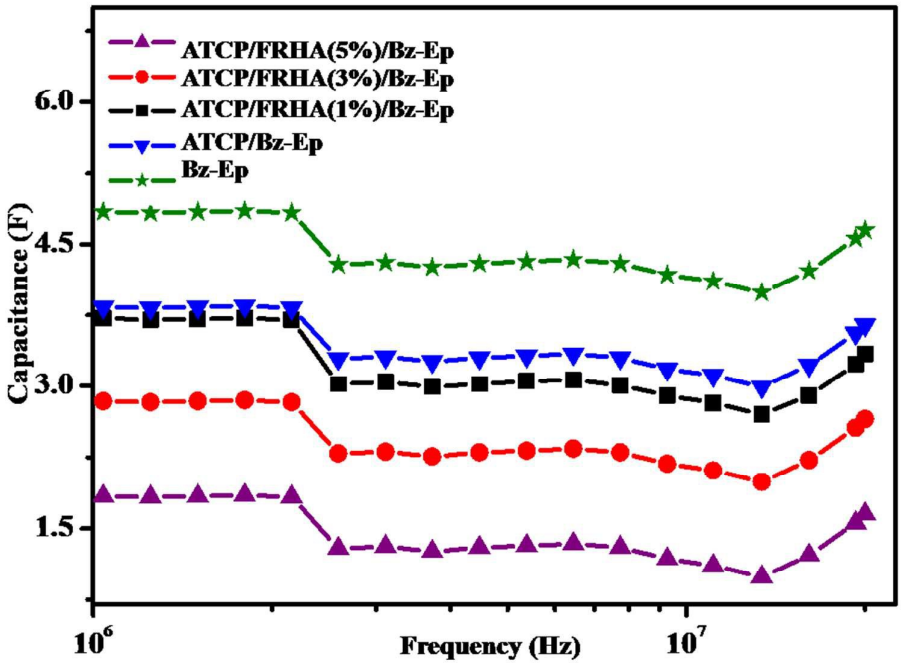

Figure 11. Dielectric constant of Bz-Ep, ATCP/Bz-Ep, ATCP/FRHA(1%)/Bz-Ep, ATCP/FRHA(3%)/Bz-Ep and ATCP/FRHA(5%)/Bz-Ep composites.

Further, the polybenzoxazine network structure constructed via multiple cross links and subsequent hydrogen bonding (–OH…O inter and –OH...N intramolecular hydrogen bonds), which may be the reason for the observed dielectric features [23-25]. These inter and intra molecular hydrogen bonding can influences the change in polarization throughout the polymer network. In addition, the intermolecular hydrogen bonding obviously can enhance the polarization and dielectric constant, whereas the intramolecular hydrogen bondings are offered the benefits to reduce the dielectric constant [25]. Further, the composites have higher volume fraction of intramolecular hydrogen bonding, which can facilitate to reduce the interfacial polarizability and hence the dielectric constant values were get reduced. In addition to that ATCP/FRHA/Bz-Ep hybrid composites have siloxane and high cross linking structure, which can also decrease the dielectric constant and dielectric loss.

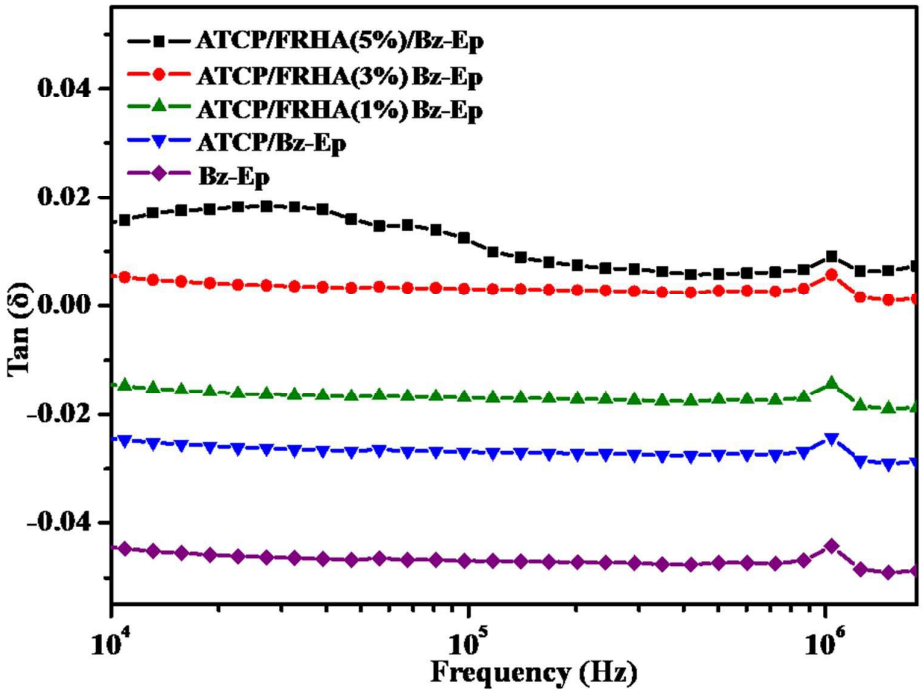

Figure 12. Dielectric loss of Bz-Ep, ATCP/Bz-Ep, ATCP/FRHA(1%)/Bz-Ep, ATCP/FRHA(3%)/Bz-Ep and ATCP/FRHA(5%)/Bz-Ep composites.

The dielectric loss is another important factor to apply the material for commercial microwave electronic devices. Almost negligible dielectric loss is desirable for practical applications. Frequency dependent dielectric loss spectra of Bz-Ep, ATCP/Bz-Ep, ATCP/FRHA(1%)/Bz-Ep, ATCP/FRHA(3%)/Bz-Ep and ATCP/FRHA(5%)/Bz-Ep composites were shown in **Figure 12** and their resulted values were presented in the **Table 2**. As similar to the dielectric constant, the values of dielectric loss were also follow the decreasing trend from Bz-Ep to ATCP/FRHA/Bz-Ep and their results were presented in **Table 2**. ATCP/FRHA/Bz-Ep system have low dielectric constant, which are due to high cross linking density, siloxane structure, intramolecular hydrogen bonding and reduces surface free energy that promotes the hydrophobic nature [26, 27] of the composites.

Apart from this, the dielectric constants are mainly depends on the polarizability of the materials and materials with less polar functional groups favour for low k value. Furthermore, the incorporation of less polar Si-O-Si contain rice husk ash is also contributed

to reduce the dielectric constant. In addition, the cross links in ATCP/FRHA/Bz-Ep maintain the sufficient distance between the matrix, which can reduce the interfacial polarization significantly that results a very low k value for the hybrid polymer system. The phenomenon such as less polar functional groups, large volume fraction of intramolecular hydrogen bonding, and low surface free energy, etc., were contributed to ATCP/FRHA/Bz-Ep composites, which are responsible for low dielectric constant value (1.62 δ) with high thermal stability as well as flame retardant. So the resultant ATCP/FRHA(5%)/Bz-Ep composite has low k value, which can be used for high performance dielectric applications.

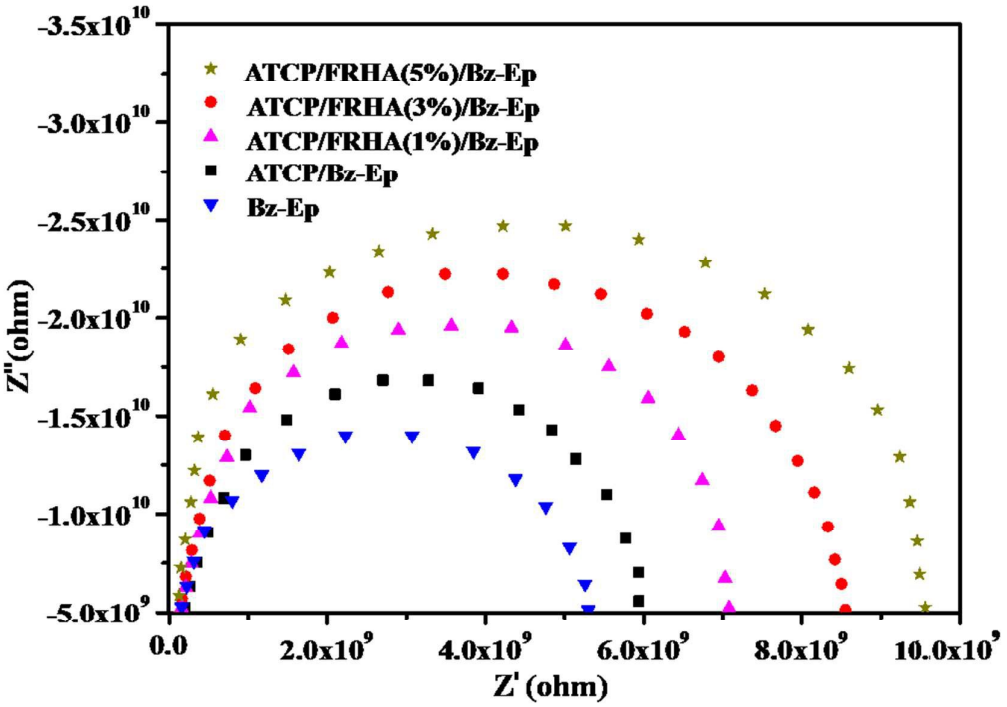

Figure 13. Nyquist plot of Bz-Ep, ATCP/Bz-Ep, ATCP/FRHA(1%)/Bz-Ep, ATCP/FRHA(3%)/Bz-Ep and ATCP/FRHA(5%)/Bz-Ep flame retardant composites.

Impedance measurements were used to assess the dielectric behaviour of the polymer composites. From the Nyquist plot **(Figure 13)**, typical capacitance response was observed with semicircle for Bz-Ep, ATCP/Bz-Ep and ATCP/FRHA(1%)/Bz-Ep, ATCP/FRHA(3%)/Bz-Ep and ATCP/FRHA(5%)/Bz-Ep composites. The large semicircle is

related to high charge transfer resistance (R_{ct}) and constant phase element (CPE_2). The sizes of semicircles were decreased, which indicates the lower electrical resistivity due to creation of conductive paths. This technique is based on the consideration of a linear electrical behaviour of the system under study. However, it has been reported that polymeric composites can also show a non-linear electrical behaviour [28, 29]. From this plot, it was noticed that the charge transfer resistance values were 5.27×10^9, 5.95×10^9, 7.11×10^9 and $9.55\times10^9\Omega$ for Bz-Ep, ATCP/Bz-Ep and ATCP/FRHA(1%)/Bz-Ep, ATCP/FRHA(3%)/Bz-Ep and ATCP/FRHA(5%)/Bz-Ep composites, respectively (Table 2). From the results, it was concluded that the ATCP/FRHA(5%)/Bz-Ep composites exhibit higher charge transfer resistances (R_{ct}) than the Bz-Ep composite**.**

Table 2

The dielectric constant, dielectric loss, charge transfer resistance and contact angle values of flame retardant composites.

Sample name	Dielectric Constant	Dielectric loss	Charge transfer resistance	Contact angle value
Bz-Ep	4.63	0.215	$5.27\times10^9\Omega$	68°
ATCP/Bz-Ep	3.64	0.194	$5.95\times10^9\Omega$	82°
ATCP/FRHA(1%)/Bz-Ep	3.32	0.173	$7.11\times10^9\Omega$	86°
ATCP/FRHA(3%)/Bz-Ep	2.65	0.135	$8.52\times10^9\Omega$	98°
ATCP/FRHA(5%)/Bz-Ep	1.62	0.091	$9.55\times10^9\Omega$	106°

Thermal properties

The glass transition temperature (T_g) of Bz-Ep ATCP/Bz-Ep, ATCP/FRHA(1%)/Bz-Ep, ATCP/FRHA(3%)/Bz-Ep and ATCP/FRHA(5%)/Bz-Ep composites were performed by DSC measurements and the data obtained were listed in the **Table 3**. The Bz-Ep matrix shows a lower T_g value than that of other ATCP/Bz-Ep, ATCP/FRHA(1, 3 & 5%)/Bz-Ep

composites (**Figure 14**). The increased value of T_g for ATCP/FRHA/Bz-Ep composites are may be due to the presence of high cross linking density among the amine terminated cyclophosphazene, functionalized rice husk ash (existence of thermally stable Si-O-Si skeleton in the composite) and benzoxazine based epoxy composites [30]. Therefore introduction of rigid groups in to the backbone of a benzoxazine based epoxy composites can increase the T_g value of the resulted cured composites.

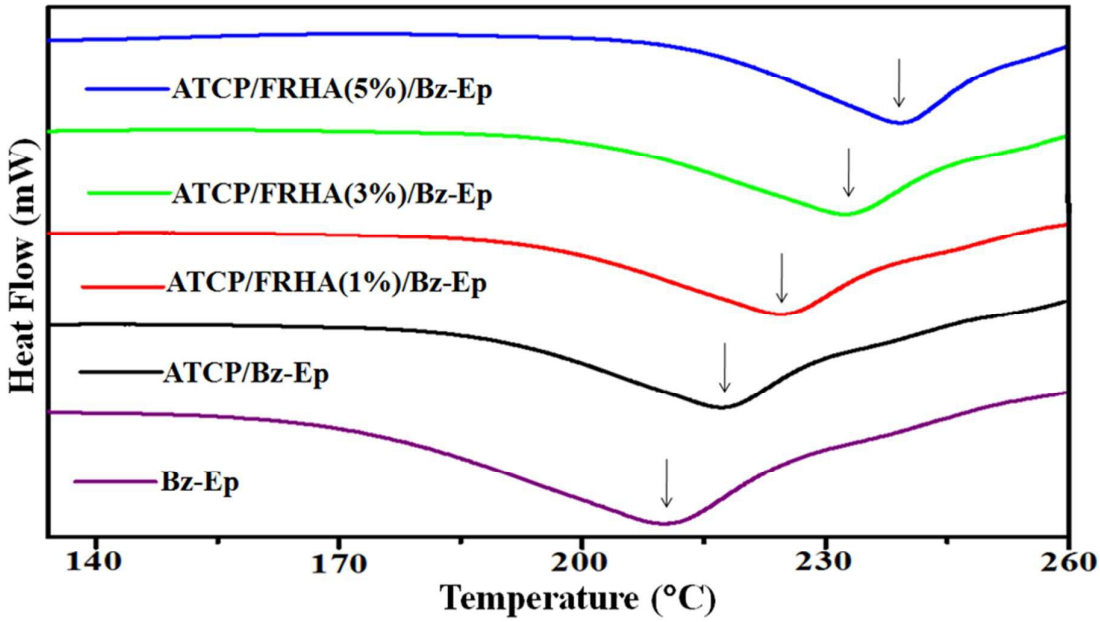

Figure 14. DSC analysis of Bz-Ep, ATCP/Bz-Ep, ATCP/FRHA(1%)/Bz-Ep, ATCP/FRHA(3%)/Bz-Ep and ATCP/FRHA(5%)/Bz-Ep flame retardant composites.

Thermogravimetric analysis (TGA) technique is another powerful tool to evaluate the thermal stability of composites. TGA of cured benzoxazine based epoxy composites can provide important information about their thermal stability and thermal degradation behavior. **Figures 15 and 16** show the TGA thermograms and DTG curves of hybrid composites in the nitrogen atmosphere and the results were presented in table 3. The 5% weight loss temperature of Bz-Ep, ATCP/Bz-Ep, ATCP/FRHA(1%)Bz-Ep, ATCP/FRHA(3%)/Bz-Ep and ATCP/FRHA(5%)/Bz-Ep composites were 318, 322, 328, 333 and 338°C, respectively. The variation in degradation values were observed, which are due to presence of phosphorous

and nitrogen containing amine terminated cyclophosphazene and silicon containing functionalized rice husk ash in the epoxy composites. Similar trend have also been observed for maximum weight loss (**Figure 16**) of the composites. Further, it was noticed that the presence of amine terminated cyclophosphazene and increasing weight percentages of functionalized rice husk ash can increase the thermal stability of the resulting composites. The decomposition temperature of phosphorus containing composites are higher than that of the conventional epoxy matrices, which is due to the presence of P–C bonds, Since the P-C bond has higher thermal stability than that of C–C bonds [31]. The major weight loss observed above 300^{o}C, which are associated with the decomposition of polymer network and finally yield residual chair at 800^{o}C.

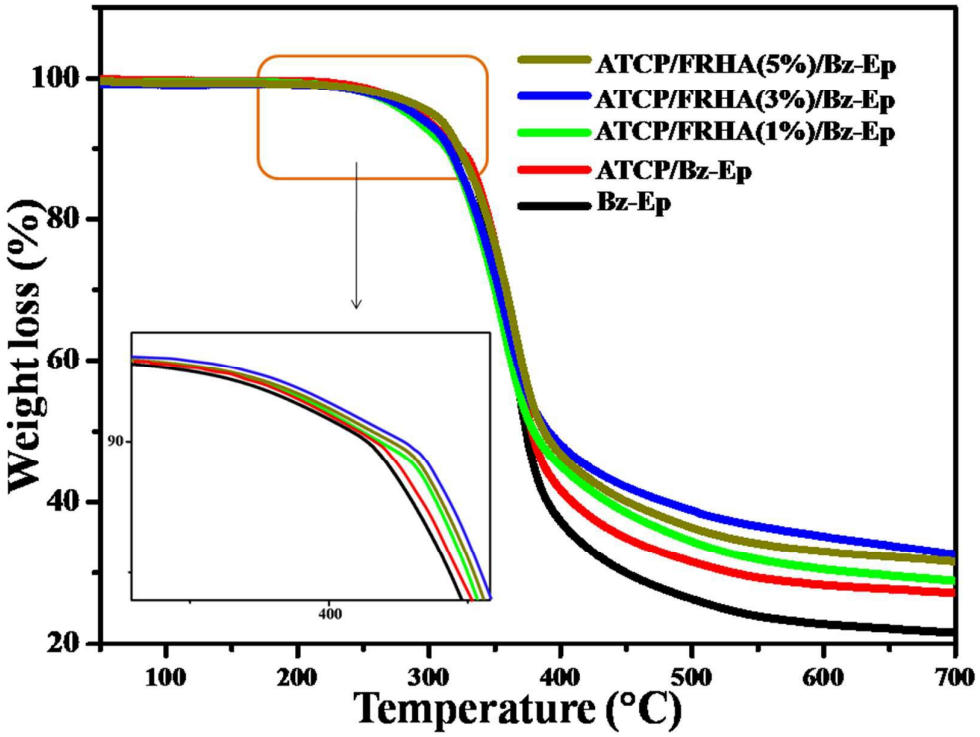

Figure 15: TGA analysis for Bz-Ep, ATCP/Bz-Ep, ATCP/FRHA(1%)/Bz-Ep, ATCP/FRHA(3%)/Bz-Ep and ATCP/FRHA(5%)/Bz-Ep flame retardant composites under nitrogen atmosphere.

From the **Table 3,** it can be seen that the value of char yield increases with increasing in wt.% of reinforcement, which are due to the presence of phosphorous, nitrogen and (1, 3 and 5%) silicon in the composite systems. A relatively higher char yield is obtained for ATCP/Bz-Ep/FRHA(5%) composite compared to that of Bz-Ep composite. Further, the higher char yield confirms higher flame retardant properties. Hence, the introduction of phosphorous, nitrogen and silicon in the modified Bz-Ep shows better flame retardancy than that of neat Bz-Ep matrix. Data obtained from thermal analysis indicate that ATCP/FRHA/Bz-Ep composites exhibit higher thermal stability and better flame retardancy than those of benzoxazine based epoxy matrix.

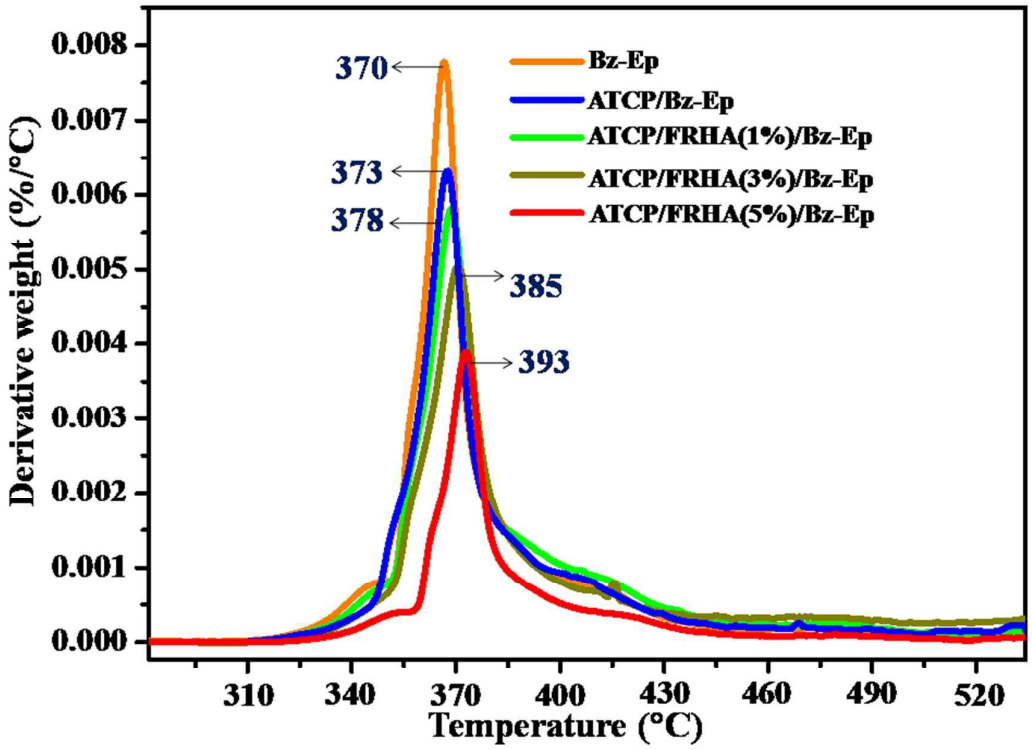

Figure 16. DTG curve of Bz-Ep, ATCP/Bz-Ep, ATCP/FRHA(1%)/Bz-Ep, ATCP/FRHA(3%)/Bz-Ep and ATCP/FRHA(5%)/Bz-Ep flame retardant composites.

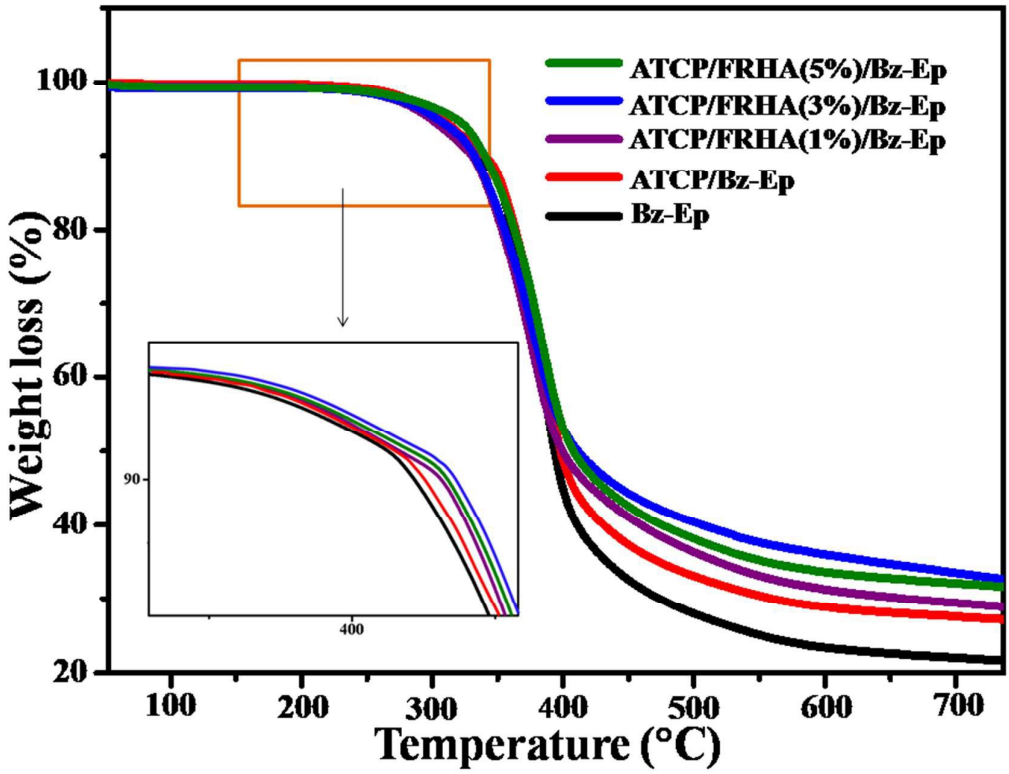

Figure 17. TGA curves of Bz-Ep, ATCP/Bz-Ep, ATCP/FRHA(1%)/Bz-Ep, ATCP/FRHA (3%)/Bz-Ep and ATCP/FRHA(5%)/Bz-Ep flame retardant composites in air atmosphere.

Table 3

Thermal properties of Bz-Ep, ATCP/Bz-Ep, ATCP/FRHA(1%)/Bz-Ep, ATCP/FRHA (3%)/Bz-Ep and ATCP/FRHA(5%)/Bz-Ep composites.

Thermoset sample	T_g (°C)	TGA in Nitrogen atmosphere			TGA in air atmosphere		
		T_{onset}[a] (°C)	T_{max}[b] (°C)	Char yield at 800°C (wt.%)	T_{onset}[a] (°C)	T_{max}[b] (°C)	Char yield at 800°C (wt.%)
Bz-Ep	211	318	370	22.57	313	367	20.84
ATCP/Bz-Ep	218	322	374	29.47	317	370	24.97
ATCP/FRHA(1%)/Bz-Ep	223	328	378	30.42	325	374	28.64
ATCP/FRHA(3%)/Bz-Ep	233	333	385	39.46	329	382	34.54
ATCP/FRHA(5%)/Bz-Ep	240	338	393	44.25	334	390	41.20

[a] The onset decomposition temperature at which the thermoset undergoes 5 wt.% of weight loss.
[b] The characteristic temperature at which maximum rate of weight loss of 40 wt.% occurs.

The TGA curves of Bz-Ep, ATCP/Bz-Ep, ATCP/FRHA(1%)/Bz-Ep, ATCP/FRHA(3%)/Bz-Ep and ATCP/FRHA(5%)/Bz-Ep flame retardant composites in the air atmosphere were shown in **Figure 17.** The decomposition processes of flame retardant composites in an air atmosphere were similar to N_2 atmosphere.

Flame retardant properties

The flammability characteristics of the composites were evaluated by UL-94 vertical burning experiment, LOI values and their results were tabulated in **Table 4**. From the results, it was noticed that the prepared composites achieved the V-0 classification except Bz-Ep composite and their corresponding LOI values were increased from 28 to 51 %. On the basis of these results, it was evidence that the ATCP and FRHA containing Bz-Ep have a virtually non-flammable nature. Such good inherent flame retardancy is ascribed to the presence of a unique combination of phosphorous, nitrogen and siloxane network in ATCP and rice husk ash incorporated Bz-Ep materials. The occurrence of above inorganic elements can promote the formation of intumescent carbonaceous char, which enhance the flame retardancy in the way of a condensed phase. Such a category of a flame retarding mechanism is well known as an intumescent mechanism. Following with this mechanism, an organic material can swell up when exposed to fire or heat to form a foamed mass usually carbonaceous in the condensed phase promoting char formation on the surface as a barrier to inhibit gaseous products from diffusing to the flame and to shield the polymer surface from heat.

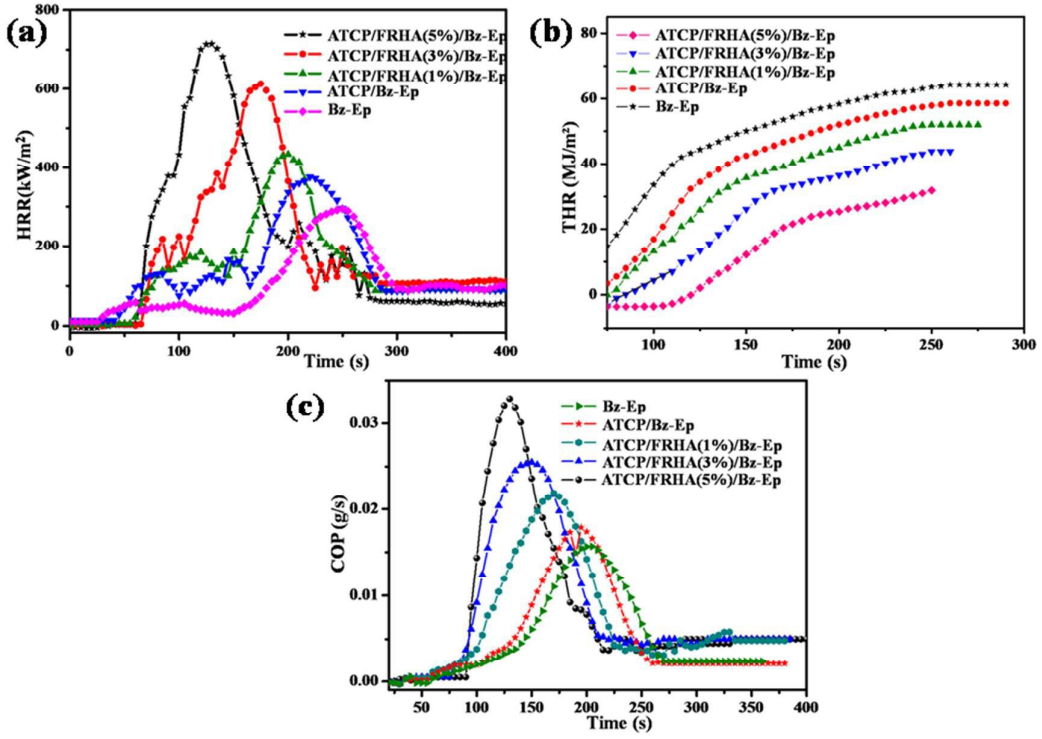

Figure 18. (a) Heat release rate (HRR), (b) total heat release rate (THR) and (b) carbon monoxide production (COP) of Bz-Ep, ATCP/Bz-Ep, ATCP/FRHA(1%)/Bz-Ep, ATCP/FRHA(3%)/Bz-Ep and ATCP/FRHA(5%)/Bz-Ep composites.

Cone calorimeter is often used to evaluate the fire resistance behaviours of materials and their measurements provide several useful burning parameters [32-37]. **Figures 18 and 19** show time to ignition (TTI), the heat release rate (HRR), total heat release rate (THR), total smoke production (TSP), carbon monoxide production (COP), and smoke production rate (SPR) for Bz-Ep, ATCP/Bz-Ep, ATCP/FRHA(1%)/Bz-Ep, ATCP/FRHA(3%)/Bz-Ep and ATCP/FRHA(5%)/Bz-Ep composites. Time to ignition was used to determine the influence on ignitability, which can be measured from the onset of HRR curve (**Table 4**). TTI showed clear differences in the ignition behaviour among the developed composite materials and TTI of the cured ATCP/FRHA(5%)/Bz-Ep system was smaller than that of Bz-Ep thermosets, which may be due to the presence of flame retarded ATCP and FRHA (**Table 4**) in the composite materials.

HRR is a measurement of heat release per unit surface area of a burning specimen. This is considered as a typical case for thin noncharring materials. The ATCP/FRHA/Bz-Ep composites show significant flame retardant effects with a drastic decrease in peak heat release rate (PHRR) from 713 to 289 KW/m^2. The combination of amine terminated cyclophosphazene (ATCP) and functionalized rice husk ash (FRHA) lead to the improvement in the flame retardant performance of the materials when compared with Bz-Ep and ATCP/Bz-Ep composites.

The peak originates from the full heat releasing of the insulating layer on the surface of the polymer composite. Here, the phosphorus groups form an insulating protective layer which prevents the volatiles transferring to the surface of the materials that increases the thermal stability of the char at higher temperatures. Further, nitrogen in polymers can release non-flammable gases or decompose endothermically to cool the pyrolysis zone at the combustion surface [38], and silicon in the FRHA are ascribed to form thermally stable silica that have the tendency to migrate on to the char surface, which is serving as a protection layer to prevent further degradation of char at high temperatures [39, 40].

Figure 18 (b) shows the total heat release (THR) curves of typical flame retarded composites. The ATCP/FRHA(5%)/Bz-Ep shows the lowest THR value among all flame retardant samples, which further evidences for good flame retardant performance. The decrease in THR value of ATCP/FRHA(5%)/Bz-Ep composite indicates that the part of the polymer is not completely burnt. Hence, the compact protective layers on the surface are serving as a thermal insulation layer that can inhibit polymer pyrolysis, the evolution of combustible gases to feed the flame and to separate the oxygen from burning materials [41].

The evolution of smoke is considered as another important parameter in the halogen-free flame retardant materials. The formation of CO in fires takes place at low temperatures in the early stage of fire development, which are primarily attributed to incomplete combustion

of the pyrolyzed polymer volatile products. When the fire develops, the higher temperature favours the formation of CO_2, which is particularly dependent on oxygen availability to the fire [42]. **Figure 18(c)** shows the CO releasing rate during combustion of composites. It can be seen that the CO productions of the flame retardant ATCP/FRHA(5%)/Bz-Ep sample is much lower than that of Bz-Ep composites during combustion.

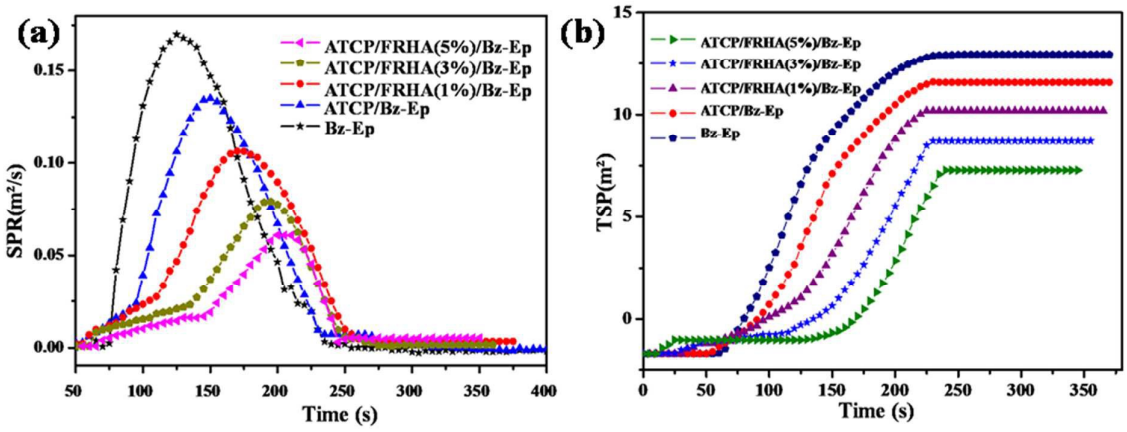

Figure 19 (a) smoke production rate (SPR) and (b) total smoke production (TSP) of Bz-Ep, ATCP/Bz-Ep, ATCP/FRHA(1%)/Bz-Ep, ATCP/FRHA(3%)/Bz-Ep and ATCP/FRHA(5%) /Bz-Ep flame retardant composites.

Table 4

Cone calorimeter and UL - 94 vertical burning test results of flame retardant composites

Sample Names	UL-94 Test	LOI Value (%)	TTI (s)	PHRR (KW/m^2)	THR (MJ/m^2)	PCOP (g/s)	PSPR (m^2/s)	TSP (m^2)
Bz-Ep	V-1	28	57	713	64	0.033	0.16	12.98
ATCP/Bz-Ep	V-0	34	52	610	58	0.025	0.13	11.33
ATCP/FRHA(1%)/Bz-Ep	V-0	39	48	435	51	0.021	0.10	8.77
ATCP/FRHA(3%)/Bz-Ep	V-0	45	45	374	43	0.017	0.07	7.36
ATCP/FRHA(5%)/Bz-Ep	V-0	51	40	289	31	0.013	0.05	5.52

To develop the flame retardant materials with low smoke polymers are the long pursued target **(Figure 19(a))**. The ATCP/FRHA(5%)/Bz-Ep sample has a much lower smoke production rate than that of other Bz-Ep composite. From the results it was concluded that the accumulation of ATCP intumescent flame retardant together with FRHA near the regressing sample surface acts as not only a heat insulation layer, but also as a barrier that prevents the decomposed volatile products migrating to the sample surface.

Analysis of residual char

SEM micrographs of outside and the inside feature of the char obtained from UL-94 test were shown in **Figures 20 and 21**. The outside aspect of the char was observed to present a carbonaceous structure with more compact and sense char layer, while the inside shows a multipores structure.

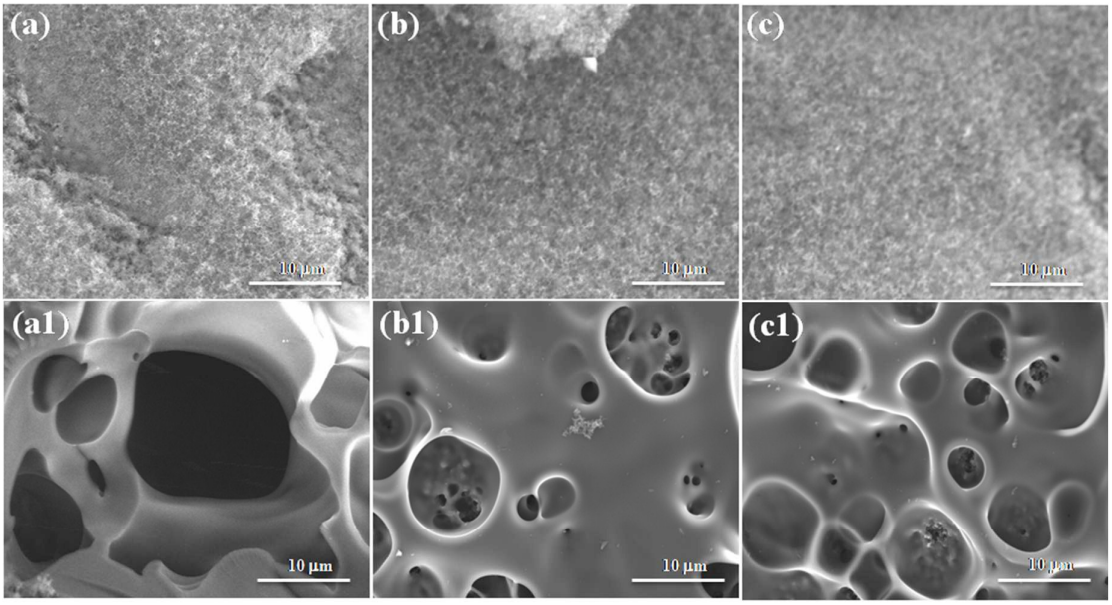

Figure 20. Char morphology and inner layer morphology of Bz-Ep (a) & (a1), ATCP/Bz-Ep (b) & (b1) and ATCP/FRHA(1%)/Bz-Ep (c) & (c1) flame retardant composites.

This result indicates a typical morphology associated with the intumescent char formation. It was well known that the charring structure is one of the most important factors that are determining the flame retardancy on the basis of SEM observation. The char layer

looks like rigid and compact with lots of integrated closed honeycomb pores in the inside structural feature that could impart a temperature grad to char layer during combustion. Such a protective char layer can serve as a barrier against heat and oxygen diffusing items that protects the inside matrix. From the FE-SEM images, it was concluded that the use of cyclophosphazene and rice husk ash as flame retardant material can lead to remarkable important flame retardant properties of resultant composite materials.

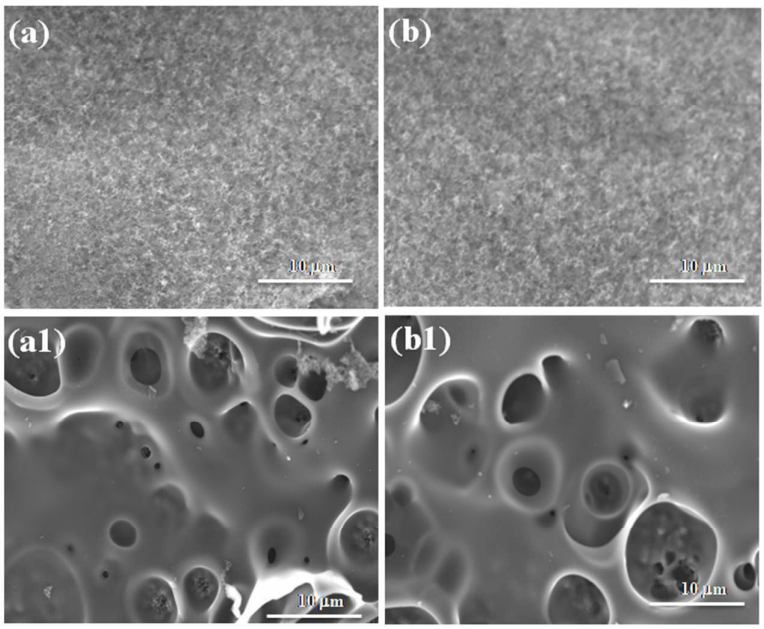

Figure 21. Char morphology and inner layer morphology of ATCP/FRHA(3%)/Bz-Ep (a) & (a1) and ATCP/FRHA(5%)/Bz-Ep (b) & (b1) flame retardant composites.

Figure 22 shows the FTIR spectra of the residual chars collected from the UL-94 test of Bz-Ep, ATCP/Bz-Ep, ATCP/FRHA(1%)/Bz-Ep, ATCP/FRHA(3%)/Bz-Ep and ATCP/FRHA(5%)/Bz-Ep. The peak observed at 3433 cm^{-1} is corresponding to NH stretching vibrations. The peaks appeared at 2961 and 2865 cm^{-1} are corresponding to C-H stretching vibrations. The peak observed at 1041cm^{-1} confirms the presence of C-O stretching vibrations. The aromatic C-C stretching vibration was observed at 1514 cm^{-1}. The characteristic stretching vibrations were observed at 1257 cm^{-1}, 1186 cm^{-1} and 946 cm^{-1} suggested that P-O-Ph, P-N-P and P-O-C bond exist in the residual chars of all tested

thermosets. Furthermore the peak observed between 1000 to 1130 cm^{-1} confirms the presence of Si-O-Si bond. From the overall results, it was concluded that the synergistic effect were occurred and it was strengthened with increasing FRHA mass ratio, which plays a very important role in self-extinguishing performance of flame retardant ATCP/FRHA/Bz-Ep composites.

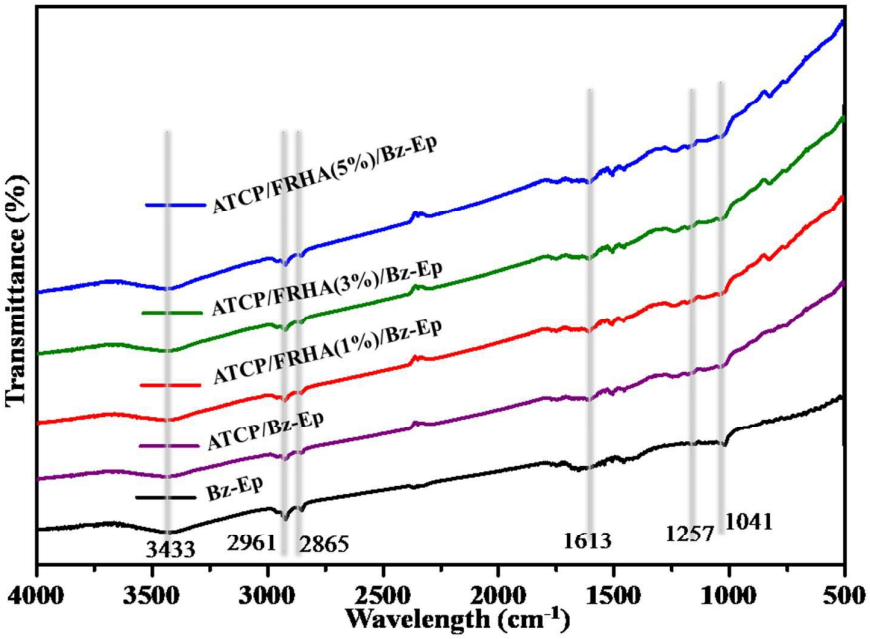

Figure 22. FT-IR spectra of residues obtained from the UL-94 test.

Figure 23 shows the digital photos of Bz-Ep, ATCP/Bz-Ep, ATCP/FRHA(1%)/Bz-Ep, ATCP/FRHA(3%)/Bz-Ep and ATCP/FRHA(5%)/Bz-Ep residues obtained after carrying out the vertical burning test. During the UL-94 vertical burning flame retardant test, all specimens were ignited with an alcohol lamp for 30s. The amount and shape of residues formed during combustion were clearly observed. Figure 23(a) shows that a rare char was formed, which confirms the poor flame retardancy and melt dripping. Figure 23(e) shows that a char layer was formed and the thickness of this char layer increased with increasing mass ratio of ATCP and FRHA materials.

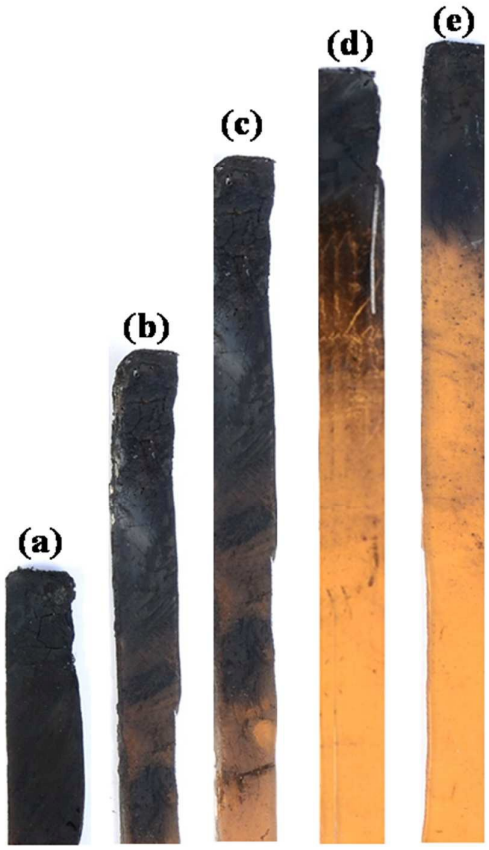

Figure 23. Digital photos of Bz-Ep, ATCP/Bz-Ep, ATCP/FRHA(1%)/Bz-Ep, ATCP/FRHA(3%)/Bz-Ep and ATCP/FRHA(5%)/Bz-E residue obtained after carrying out UL-94 vertical burning flame retardant test.

Conclusion

In this paper, ATCP and FRHA were utilized together as a novel combined halogen free flame retardant system to improve the flame retardance of benzoxazine blended epoxy composites. The addition of FRHA enhances both flame retardance and dielectric properties of amine terminated cyclophosphazene reinforced benzoxazine based epoxy matrix. The fracture surface exhibit a non-phase separated platelet like homogeneous morphology. The dielectric constant and loss were decreased due to presence of intramolecular hydrogen bonding, high cross linking density and orientation of the molecule. The improvement in the electrical resistivity was confirmed by nyquist plot with high charge transfer resistance of composite materials. The improved hydrophobic nature was confirmed by contact angle

measurements. Further, the introduction of small amount of ATCP and FRHA were accelerated to improve the degradation properties, which are leading to a compact and unbroken N, P and Si protective layer. Therefore, drastically depressed peak heat release rates were achieved. This novel flame retardant composite will pave a new possibility for high performance halogen free flame retardant polymeric materials, which could be applied for micro-electronic devices.

Acknowledgement

The authors like to thank DST/Nanomission, New Delhi, India for financial support to carry out this work and to establish Nanotech Research Lab through the grant No. SR/NM/NS-05/2011(G).

References

1. A. Riva, G. Camino, L. Fomperie and P. Amigouet, *Polym. Degrad. Stab.*, 2003, **82**, 341.
2. M. Fu and B. Qu, *Polym. Degrad. Stab*., 2004, **85**, 633.
3. S. M. El-Sayed, H. M. Abdel Hamid and R. M. Radwan, *Radiat. Phys. Chem.,* 2004, **69**, 339.
4. Junwei Gu, Qiuyu Zhang, Jing Dang and Chao Xie, Polymers for Advanced Technologies, 2012, **23**, 1025.
5. Junwei Gu, Jing Dang, Yalan Wu, Chao Xie and Ying Han, Polymer Plastics Technology and Engineering, 2012, **51**, 1198.
6. Jun-wei Gu, Guang-cheng Zhang, Shan-lai Dong, Qiu-yu Zhang and Jie Kong, Surface and Coatings Technology, 2007, **201**, 7835.
7. G. C. Stevens and A. H. Mann, Risks and benefits in the use of flame retardants in consumer products: a report for the Department of trade and industry. Surrey: University of Surrey, Polymer Research Centre; 1999.
8. H. Ishida and T. Agag, Elsevier, Amsterdam, 1nd edn, 2011, ch. 7, 169.
9. S. Rimdusit and H. Ishida, Polymer, 2000, 41, 7941.
10. S. Tragoonwichian, N. Yanumet and H. Ishida, *J. Appl. Polym. Sci.,* 2007, **106**, 2925.

11. H. R Allcock, Chemistry and applications of phosphazenes, wiley-interscience: Hoboken, NJ, 2003,19.
12. S. Fei and H. R. Allcock, *J Power Sources,* 2010, **195**, 2082.
13. H. R. Allcock, *J Inorg Organomet Polym Matter,* 2006, **16**, 277.
14. J. Ding and W. Shi, *Polym. Degrad. Stab.,* 2004, **84**, 159.
15. D. Kumar, G. M. Fohlen and J. A. Parker, *Macromolecules* 1983, **16**, 1250.
16. I. Apivhat, P. Eakachai, *J. Hazardous Mater*, 2010, **184**, 775.
17. K. Krishnadevi, A. Nirmala Grace, M. Alagar and V. Selvaraj, *High Perform. Polym,* 2014, **26**, 1.
18. K. Krishnadevi, V. Selvaraj, and D. Prasanna, RSC Advances, 2015, **5**, 913.
19. H. Ishida, D. P. Sanders. *Macromolecules,* 2000, **33**, 8149.
20. Ezzat Rafiee, Shabnam Shahebrahimi, Mostafa Feyzi and Mahdi Shaterzadeh, International Nano Letters, 2012, **2**, 29.
21. A. Proctor, P. K. Clark and C. A. Pareker, *J. Am. Oil. Chem So.c,* 1995, **72**, 459.
22. M. Rozainee, S. P. Ngo, S. S. Slem, K. G. Tan, M. Ariffin and Z. N. Zainura, *Bioresour. Technol*, 2008, **99**, 703.
23. J. Fan, X. Hu and C.Y Yue, *J Polym Sci B Polym Phys*, 2003, **41**, 1123.
24. H. D. Kim and H. Ishida, *J. Phys. Chem. A,* 2002, **106**, 3271.
25. C. F. Wang, Y. C. Su, S. W. Kuo, C. F. Huang, Y. C. Sheen, and F. C. Chang, *Angew. Chem. Int. Ed.,* 2006, **45**, 2248.
26. C. S. Liao, C. F. Wang, H. C. Lin, H. Y. Chou, and F. C. Chang, *Langmuir*, 2009, **25,** 3359.
27. J. Liu, X. Lu, Z. Xin, and C. Zhou, *Langmuir,* 2013, **29**, 411.
28. T. Alizadeh, *Mater.Chem.Phys,* 2012, **135**, 1012.
29. J. Guo, A. Sun, X. Chen, C. Wang and A. Manivannan, *Electrochim.Acta,* 2011, **56**, 3981.
30. M. Sponton, L. A. Mercado, J. C. Ronda, M. Galia and V. Cadiz, *Polym Degad Stabil.,* 2008, **93**, 2025.
31. U. Quittmann, L. Lecamp, W. E. Khatib, B. Youssef, and C. Bunel, *Macromol Chem Phys*, 2001, **202**, 628.
32. A. B.Morgan and M. Bundy, *Fire Mater.,* 2007, **31**, 257.
33. C. Siat, M. L. Bras and S. Bourbigot, *Fire Mater.* 1998, **22**, 119.
34. B. Schartel and T. R. Hull, *Fire Mater.* 2007, **31**, 327.

35. G. Gallina, E. Bravin, C. Badalucco, G. Audisio, M. Armanini, A. D. Chirico and F. Provasoli, *Fire Mater.* 1998, **22**, 15.
36. D. Y. Wang, Y. Liu, Y. Z. Wang, C. P. Artiles, T. R. Hull, and D. Price, *Polym. Degrad. Stab.* 2007, **92**, 1592.
37. P. J. Elliot and R. H. A. Whiteley, *Polym. Degrad. Stab.* 1999, **64,** 577.
38. F. Gao, L. Tong anad Z. Fang, *Polym. Degrad. Stab*, 2006, **91**, 1295.
39. L. Y. Ling, W. W. Lung, H. K. Ying and H. W. Hsuan, *Thermochimica Acta,* 2004, **412**, 139.
40. G. L. Nelson, *Fire retardancy of polymeric materials*, New York, Marcel Dekker, 2000, 1.
41. S. Bourbigot, M. LeBras, R. Delobel and L. Gengembre, *Appl. Surf. Sci.* 1997, **120**, 15.
42. Y. Y. Yen, H. T. Wang and W. J. Guo, *Polym. Degrad. Stab.* 2012, **97**, 863.
43. M. Z. Fu and B. J. Qu, *Polym. Degrad. Stab*. 2004, **85**, 633.